



HAL
open science

Direct and Indirect Visualization of Bacterial Effector Delivery into Diverse Plant Cell Types during Infection

Elizabeth Henry, Tania Y. Toruno, Alain Jauneau, Laurent Deslandes, Gitta Coaker

► **To cite this version:**

Elizabeth Henry, Tania Y. Toruno, Alain Jauneau, Laurent Deslandes, Gitta Coaker. Direct and Indirect Visualization of Bacterial Effector Delivery into Diverse Plant Cell Types during Infection. *The Plant cell*, 2017, 29 (7), pp.1555-1570. 10.1105/tpc.17.00027 . hal-01606044

HAL Id: hal-01606044

<https://hal.science/hal-01606044>

Submitted on 26 May 2020

HAL is a multi-disciplinary open access archive for the deposit and dissemination of scientific research documents, whether they are published or not. The documents may come from teaching and research institutions in France or abroad, or from public or private research centers.

L'archive ouverte pluridisciplinaire **HAL**, est destinée au dépôt et à la diffusion de documents scientifiques de niveau recherche, publiés ou non, émanant des établissements d'enseignement et de recherche français ou étrangers, des laboratoires publics ou privés.

Copyright



BREAKTHROUGH REPORT

Direct and Indirect Visualization of Bacterial Effector Delivery into Diverse Plant Cell Types during Infection ^{OPEN}

Elizabeth Henry,^a Tania Y. Toruño,^{a,1} Alain Jauneau,^{b,1} Laurent Deslandes,^c and Gitta Coaker^{a,2}^a Department of Plant Pathology, University of California, Davis, California 95616^b Institut Fédératif de Recherche 3450, Université de Toulouse, CNRS, UPS, Plateforme Imagerie TRI-Genotoul, Castanet-Tolosan 31326, France^c LIPM, Université de Toulouse, INRA, CNRS, UPS, Castanet-Tolosan, France

ORCID IDs: 0000-0002-9220-016X (T.Y.T.); 0000-0003-0899-2449 (G.C.)

To cause disease, diverse pathogens deliver effector proteins into host cells. Pathogen effectors can inhibit defense responses, alter host physiology, and represent important cellular probes to investigate plant biology. However, effector function and localization have primarily been investigated after overexpression in planta. Visualizing effector delivery during infection is challenging due to the plant cell wall, autofluorescence, and low effector abundance. Here, we used a GFP strand system to directly visualize bacterial effectors delivered into plant cells through the type III secretion system. GFP is a beta barrel that can be divided into 11 strands. We generated transgenic *Arabidopsis thaliana* plants expressing GFP1-10 (strands 1 to 10). Multiple bacterial effectors tagged with the complementary strand 11 epitope retained their biological function in *Arabidopsis* and tomato (*Solanum lycopersicum*). Infection of plants expressing GFP1-10 with bacteria delivering GFP11-tagged effectors enabled direct effector detection in planta. We investigated the temporal and spatial delivery of GFP11-tagged effectors during infection with the foliar pathogen *Pseudomonas syringae* and the vascular pathogen *Ralstonia solanacearum*. Thus, the GFP strand system can be broadly used to investigate effector biology in planta.

INTRODUCTION

Plants can be infected by all classes of pathogens and rely on their innate immune system to recognize and respond to invading organisms (Henry et al., 2013). An important aspect of pathogenicity is the delivery of pathogen proteins, termed effectors, into host cells (Toruño et al., 2016). Effectors can modulate host metabolism, shut down host defense signaling, and suppress cell death (Toruño et al., 2016). Gram-negative bacterial pathogens such as the foliar pathogen *Pseudomonas syringae* and the vascular pathogen *Ralstonia solanacearum* use the type III secretion system (TTSS), a proteinaceous needle-like structure, to directly deliver effectors inside host cells (Chang et al., 2014). Mutations in core components of the TTSS, such as the homopolymeric ring hC, block the ability to cause disease (Deng et al., 1998; Vasse et al., 2000). Plants have evolved intracellular immune receptors with nucleotide binding leucine-rich repeat (NLR) domain architecture that specifically recognize pathogen effectors leading to effector-triggered immunity (ETI) (Chiang and Coaker, 2015). A hallmark of ETI is the hypersensitive response (HR), a specialized form of programmed cell death. Much of our

understanding of the plant innate immune system has been gained through investigation of the model plant *Arabidopsis thaliana*, which can be infected by pathogens with diverse tissue preferences, including *P. syringae* and *R. solanacearum*.

Intracellular delivery of GFP-tagged effectors from the fungal pathogen, *Magnaporthe oryzae*, has been successfully visualized inside plant cells (Khang et al., 2010). However, this approach has not been successful for other fungal pathogens, possibly due to the GFP tag, which can interfere with effector delivery or function, or due to low-level effector expression (Tanaka et al., 2015). Despite the importance of bacterial effectors in the modulation of host-microbe interactions, direct TTSS effector delivery has not been visualized in whole organisms. Recently, delivery of the virulence protein VirE2 by *Agrobacterium tumefaciens* through the type IV secretion system was successfully visualized using the GFP strand system in yeast, *Arabidopsis*, and tobacco (*Nicotiana tabacum*; Li et al., 2014; Li and Pan, 2017; Yang et al., 2017). The type IV secretion system is responsible for delivery and uptake of proteins and DNA, with a conduit diameter of ~18.5 nm (Wallden et al., 2010). Size constraints of the inner needle (2- to 3-nm conduit) of the TTSS require proteins to be unfolded prior to secretion and fusion with a full-length fluorophore would likely block delivery (Akedo and Galán, 2005; Chang et al., 2014). Bacterial effector delivery by the TTSS has been studied indirectly in plant genotypes during ETI, via cell viability staining during the HR (Torres et al., 2002; Greenberg and Yao, 2004). However, due to the spread of defense signaling by apoplastic reactive oxygen species and potentially other small molecules that can move through plasmodesmata (including some pathogen effectors), it is

¹ These authors contributed equally to this work.² Address correspondence to glcoaker@ucdavis.edu.

The author responsible for distribution of materials integral to the findings presented in this article in accordance with the policy described in the Instructions for Authors (www.plantcell.org) is: Gitta Coaker (glcoaker@ucdavis.edu).

^{OPEN}Articles can be viewed without a subscription.

www.plantcell.org/cgi/doi/10.1105/tpc.17.00027

impossible to determine which cells are direct recipients of bacterial effectors or which host cells are capable of directly recognizing effectors (Allan and Fluhr, 1997; Torres et al., 2002; Greenberg and Yao, 2004; Khang et al., 2010). Additionally, effector detection in the host has relied primarily on overexpression in *Nicotiana benthamiana* or *Arabidopsis*, but these approaches may not reflect their subcellular localization/targeting and accumulation under natural infection. Thus, multiple questions remain regarding which cells are targeted for effector delivery and where effectors localize within the host cell during infection.

Here, we investigated cell-specific immune responses and used the GFP strand system to directly visualize the delivery of bacterial effectors in planta. This approach allowed direct visualization of the *P. syringae* effectors AvrPto, AvrPtoB, and AvrB delivered into diverse leaf cell types during natural infection and visualization of the *R. solanacearum* effector PopP2. The GFP strand system enables the investigation of effector biology during natural infection in intact plants, and our findings provide insight to the overlap of cell-type-specific immune responses and patterns of effector delivery.

RESULTS

Diverse Cell Types in Arabidopsis Leaves Recognize and Respond to the Bacterial Effector AvrB

To investigate the capacity of various leaf cell types to recognize and respond to pathogenic bacteria, cell death was used as a proxy for effector recognition. The HR was visualized using trypan blue, a vital stain that selectively accumulates in dead cells turning them blue (van Wees, 2008). In *Arabidopsis*, the RPM1 NLR immune receptor recognizes phosphorylation of the plant protein RIN4 induced in the presence of the AvrB and AvrRpm1 effectors (Chung et al., 2011; Liu et al., 2011). The RPS2 NLR immune receptor recognizes cleavage and elimination of RIN4 by the AvrRpt2 effector protease (Axtell and Staskawicz, 2003; Mackey et al., 2003). Dip inoculation of *Arabidopsis* Col-0 with virulent *P. syringae* pv *tomato* (*Pst*) DC3000 carrying an empty vector (EV) did not result in trypan blue staining of leaf cells 14 h postinoculation (hpi) (Figure 1A). In contrast, Col-0 infection with *Pst* carrying the AvrB effector resulted in activation of RPM1-mediated resistance and accumulation of the trypan blue stain in the epidermal pavement and guard cells as well as internal mesophyll cells (Figure 1A).

To probe the ability of specific cell types to elicit ETI responses, we complemented the *Arabidopsis* double mutant *rps2-101C/rin4* (*r2r4*) with genomic T7-tagged *RIN4* driven by previously published cell-specific promoters (CSPs) for guard cells (*pGC1*), epidermal cells (*pCER6*), and mesophyll cells (*pCAB3*) (Yang et al., 2008; Ranjan et al., 2011) (Figure 1B). Expression of *RIN4* in the CSP lines compared with Col-0 was determined by anti-*RIN4* immunoblotting (Supplemental Figure 1). In order to enable detection of *RIN4* in transgenic lines using different CSPs, protein loading for the Col-0 control was diluted by half to avoid overexposure. *RIN4* expression in the cell-specific transgenic lines was still less than the diluted Col-0 sample. Lines were dip inoculated with *Pst* DC3000 (*avrB*) and assessed for the ability to

elicit a microscopic HR by trypan blue staining (Figure 1B). In the *r2r4* background, RPM1 is not functional due to the absence of *RIN4* (Mackey et al., 2002). As expected, the *r2r4* line did not elicit an HR and was not stained by trypan blue, whereas the *rps2-101C* single mutant (*r2*) used as a positive control displayed an HR in all cell types (Figure 1C). When the *rin4* mutation is complemented in a cell-specific manner, single-cell HR is also detected in *RIN4*-expressing cell types using trypan blue staining (Figure 1C).

In order to visualize macroscopic HR, we infiltrated the same *Arabidopsis* genotypes with a high dose of *Pst* DC3000 (EV) or (*avrB*) (Figure 1D). After *Pst* DC3000 (*avrB*) inoculation, we could visualize macroscopic HR spread throughout the infiltrated area in all lines containing *RIN4* (Figure 1D). Infiltration with *Pst* DC3000 (EV) did not induce an HR in any lines. To quantify macroscopic HR in the CSP lines, we measured ion leakage, a proxy for cell death (Henry et al., 2015). Consistent with the limited expression of *RIN4* in different cell types, we found the ion leakage in the CSP lines was reduced with respect to the positive controls Col-0 and *r2* after infiltration with *Pst* DC3000 (*avrB*) (Figure 1E). Together, these results indicate that discrete cell types within the leaf tissue are capable of responding to recognized effectors and may propagate cell death signals across tissues either through plasmodesmata linkages or by apoplastic reactive oxygen species signaling. Alternatively, there may be a small amount of *RIN4* expressed in other cells in CSP lines that is sufficient to induce cell death after high density inoculation.

The GFP Strand System Functions in *N. benthamiana* and Effector Function Is Retained When Fused with GFP Strand 11

Although diverse cell types are able to recognize AvrB, this does not demonstrate direct bacterial effector delivery into these cells (Figure 1). To visualize bacterial effector delivery in planta, we adopted the GFP strand system based on spontaneous assembly of two complementary GFP fragments (Cabantous et al., 2005). GFP is a beta barrel protein and can be divided into 11 strands (Cabantous et al., 2005). The success of the GFP strand system for detection of type three secreted proteins was previously demonstrated for the *Salmonella* effectors PpB2 and SteA into HeLa cell culture, indicating that the strand 11 tag does not interfere with bacterial effector delivery in *Salmonella* (Van Engelenburg and Palmer, 2010). We used an optimized superfolder GFP variant, which exhibits enhanced solubility, folding, and fluorescence (Cabantous et al., 2005; Pédelacq et al., 2006). The small 16-amino acid eleventh strand (RDHMLVLEHYVNAAGIT) was fused via a flexible linker (GDGGSGGGS) on the C terminus of the *P. syringae* effectors AvrB, AvrPto, and AvrPtoB (Figure 2A). When the effector-GFP₁₁ fusion is coexpressed with GFP₁₋₁₀, the two complementary GFP fragments should spontaneously associate/self-assemble to form a functional GFP molecule (Figure 2A). First, we demonstrated proof of concept for the GFP strand system using *Agrobacterium tumefaciens*-mediated transient plant expression system in *N. benthamiana*. GFP₁₋₁₀ and the individual effector-GFP₁₁ constructs were transiently expressed in *N. benthamiana* cells (Figure 2B). Expression of GFP₁₋₁₀ alone did not result in fluorescence, whereas coexpression with effector-GFP₁₁ resulted in clear GFP fluorescence (Figure 2B).

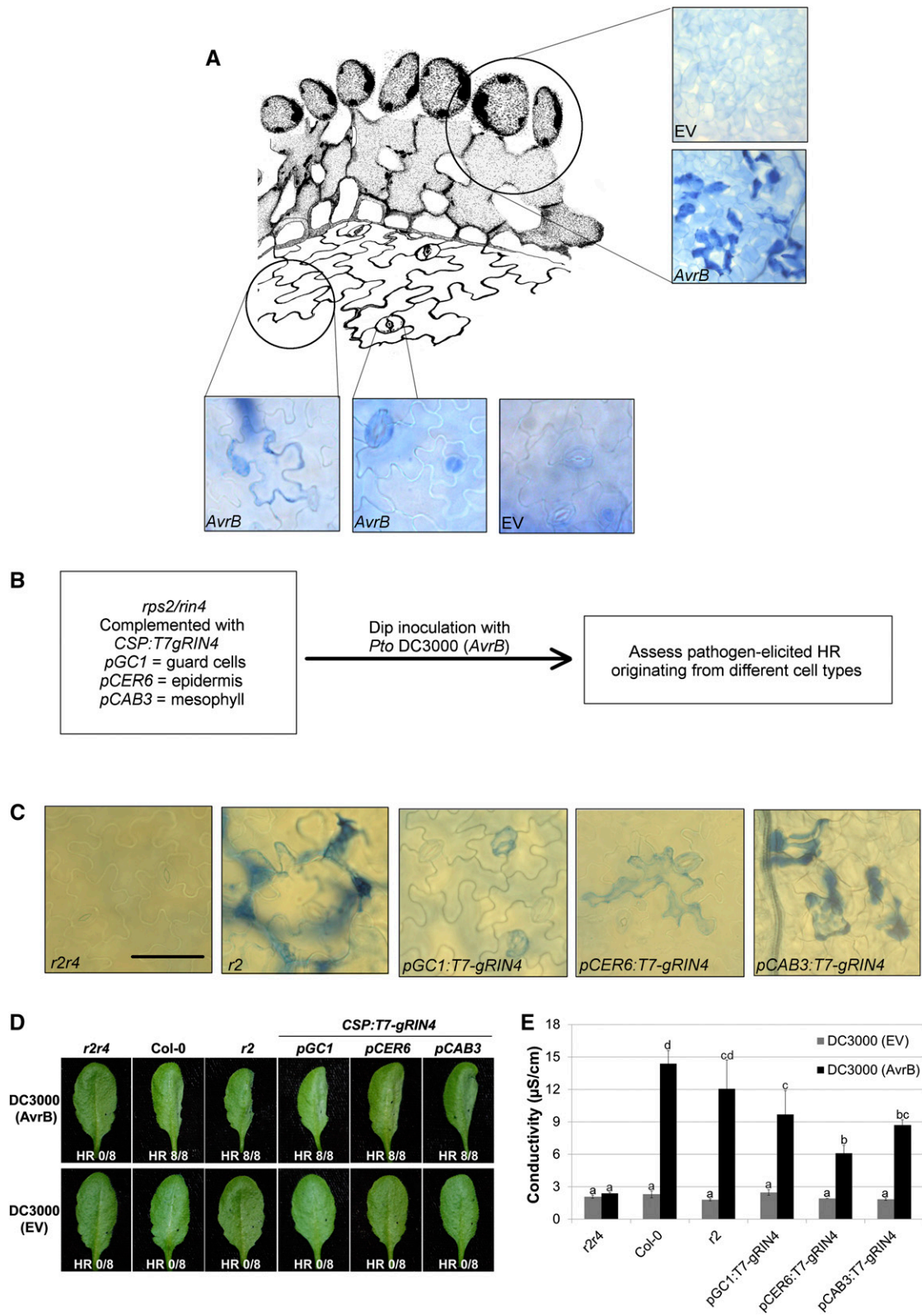


Figure 1. Cell-Specific Immune Responses in Plant Leaves.

(A) All leaf cell types are able to elicit cell death upon effector recognition. Four-week-old *Arabidopsis* Col-0 plants were dip inoculated with *Pst* DC3000 expressing EV or the bacterial effector *avrB*. Twelve hours postinoculation, microscopic cell death was visualized using trypan blue staining. Circles indicate representative trypan blue staining in leaf mesophyll, epidermal, and guard cells elicited by recognition of *P. syringae* *avrB* but not by inoculation with *P. syringae* EV.

Expression of full-length GFP₁₋₁₁ also resulted in clear fluorescence. Plasmolysis revealed that effector subcellular localization was consistent with previous reports: AvrB-GFP₁₁ and AvrPtoB-GFP₁₁ were detected at the plasma membrane with visible Hechtian strands after plasmolysis and AvrPtoB-GFP₁₁ exhibited cytosolic localization (Nimchuk et al., 2000; de Vries et al., 2006) (Figure 2B).

Pst DC3000 infects both tomato (*Solanum lycopersicum*) and Arabidopsis, causing bacterial speck disease. In resistant tomato genotypes such as the cultivar Rio Grande (RG) 76R, AvrPto and AvrPtoB both interact with tomato protein kinase Pto, which is guarded by the tomato NLR Prf (Martin et al., 1993; Salmeron et al., 1996). In the susceptible tomato genotype RG *prf3*, AvrPto and AvrPtoB promote bacterial virulence (Martin et al., 1993; Lin and Martin, 2005). In order to verify that effector fusion to GFP strand 11 does not impact effector delivery and function, inoculations were performed in tomato using *Pst* expressing AvrPto-GFP₁₁ and AvrPtoB-GFP₁₁. Effectors were cloned into the pBBR1 plasmid under the control of their native promoters and expressed with a C-terminal fusion to GFP strand 11 as described above (Kovach et al., 1995). The resulting plasmids were transformed into *Pst* DC3000. Since AvrPto and AvrPtoB are functionally redundant with respect to the host ETI response, they were singly complemented into a *Pst* double deletion mutant for both effectors (DC3000 Δ avrPto/ Δ avrPtoB) (Lin and Martin, 2005). *Pst* DC3000 Δ avrPto/ Δ avrPtoB caused disease on both RG and RG *prf3*, although symptoms were attenuated compared with wild-type *Pst* DC3000 (Figures 3A and 3B). Complementation of DC3000 Δ avrPto/ Δ avrPtoB with either AvrPto-GFP₁₁ or AvrPtoB-GFP₁₁ resulted in recovery of recognition and resistance in the RG background (Figures 3A and 3B, DC3000). Complementation of Δ avrPto/ Δ avrPtoB with AvrPto-GFP₁₁ leads to a complete recovery of virulence and bacterial titers in RG *prf3* (Figures 3A and 3B). However, complementation of *Pst* DC3000 Δ avrPto/ Δ avrPtoB with AvrPtoB-GFP₁₁ enhanced disease symptoms, but did not result in a significant increase in bacterial virulence in RG *prf3* (Figures 3A and 3B). Previously, AvrPtoB was demonstrated to enhance DC3000 disease symptoms but not bacterial titers at 4 d postinoculation (Lin and Martin, 2005). These data demonstrate that both AvrPto and AvrPtoB effectors are able to be delivered into plant cells via the TTSS and can be recognized by the plant innate immune system when fused to GFP strand 11.

In order to verify that fusion to GFP strand 11 does not impact AvrB delivery and function, inoculations were performed in Arabidopsis using *Pst* DC3000 expressing AvrB-GFP₁₁. AvrB is

recognized by the RPM1 NLR in the Arabidopsis Col-0 ecotype (Boyes et al., 1998). The ability of AvrB-GFP₁₁ to elicit RPM1-mediated responses was assessed using trypan blue staining as well as bacterial growth assays. To assess macroscopic HR, leaves of Col-0 plants were syringe infiltrated with a bacterial suspension of either *Pst* DC3000 (EV) or *Pst* DC3000 (*avrB-GFP₁₁*). Infection with *Pst* DC3000 (*avrB-GFP₁₁*) elicited a robust macroscopic HR, visualized by trypan blue at 24 hpi (Figure 3C). Bacterial growth assays demonstrate that AvrB-GFP₁₁ is delivered and recognized by RPM1, as the bacterial growth of *Pst* DC3000 (*avrB-GFP₁₁*) was attenuated at 4 d postinoculation compared with DC3000 EV on Col-0 but not the *rpm1-3* mutant line (Figures 3D and 3E). Taken together, these results indicate that effector-GFP₁₁ fusions, when delivered by the TTSS of *Pst* DC3000, are recognized by host NLR immune receptors and can promote bacterial virulence in susceptible genetic backgrounds.

Effectors Are Delivered into Multiple Cell Types in Arabidopsis Leaves

To visualize effector delivery during natural infection, we infiltrated *Pst* DC3000 strains carrying the complementary GFP strand 11 tagged effectors into homozygous transgenic Arabidopsis lines expressing 35S:*GFP₁₋₁₀* (Supplemental Figure 2). To avoid the cell death elicited by RPM1-mediated recognition of AvrB in wild-type Col-0, *rpm1-3/rps2-101C* mutant plants (*r1r2*) lacking both RPM1 and RPS2 NLR receptors expressing GFP₁₋₁₀ were used to analyze AvrB-GFP₁₁ delivery. The following *Pst* genotypes were used to detect bacterial effector delivery in the Col-0 background: DC3000 Δ avrPto/ Δ avrPtoB + *avrPto-GFP₁₁*, DC3000 Δ avrPto/ Δ avrPtoB + *avrPtoB-GFP₁₁*, DC3000 Δ avrPto/ Δ avrPtoB (negative control), DC3000 Δ hrcC + *avrPtoB-GFP₁₁* (negative control), and DC3000 Δ hrcC + *avrPto-GFP₁₁* (negative control). The following *Pst* genotypes were used to detect bacterial effector delivery in the *r1r2* background: DC3000 + *avrB-GFP₁₁*, and DC3000 EV (negative control). Confocal micrographs were acquired with the Zeiss LSM710 confocal microscope. We analyzed four different Arabidopsis plants for each bacterial strain. Two inoculation methods were assessed: syringe (Figure 4) and surface inoculation (Figure 5).

Effector delivery was first assessed after syringe inoculation of 4-week-old Arabidopsis leaves with *Pst* DC3000 carrying each of the three GFP₁₁ tagged effectors. We examined and quantified confocal micrographs taken from four biological replicates to record the temporal and spatial delivery of AvrB-GFP₁₁,

Figure 1. (continued).

(B) Complementation of specific leaf cell types with the immune regulator *RIN4* to assess cell-specific immune responses. Transgenic lines were generated expressing *RIN4* under cell specific promoters in the *rps2-101c/rin4* knockout genetic background. *r2* = *rps2-101c*; *r4* = *rin4*.

(C) Four-week-old Arabidopsis plants expressing *RIN4* in a cell-specific manner were dip inoculated with *P. syringae* (EV) and (*avrB*). Twelve hours postinoculation, trypan blue staining was used to visualize cell death in *r2r4*, *r2*, and cell-specific promoter lines. All cell types were capable of eliciting cell death after inoculation with *P. syringae* (*avrB*). Bar = 100 μ m.

(D) Four-week-old Arabidopsis plants of the indicated genotypes were subjected to half-leaf syringe infiltration with *P. syringae* DC3000 (*avrB* or EV). Eight plants per genotype were infiltrated with each bacterial strain and macroscopic cell death was recorded 16 hpi.

(E) Four-week-old Arabidopsis plants of the indicated genotypes were syringe infiltrated as described in **(D)** and ion leakage (μ S/cm) was measured with a conductivity meter 5 hpi. Bars represent means, *n* = 3 individual plants, and error bars represent sd. Statistical differences were conducted by ANOVA followed by LSD mean separation, alpha = 0.05. Experiments were repeated three times with similar results.

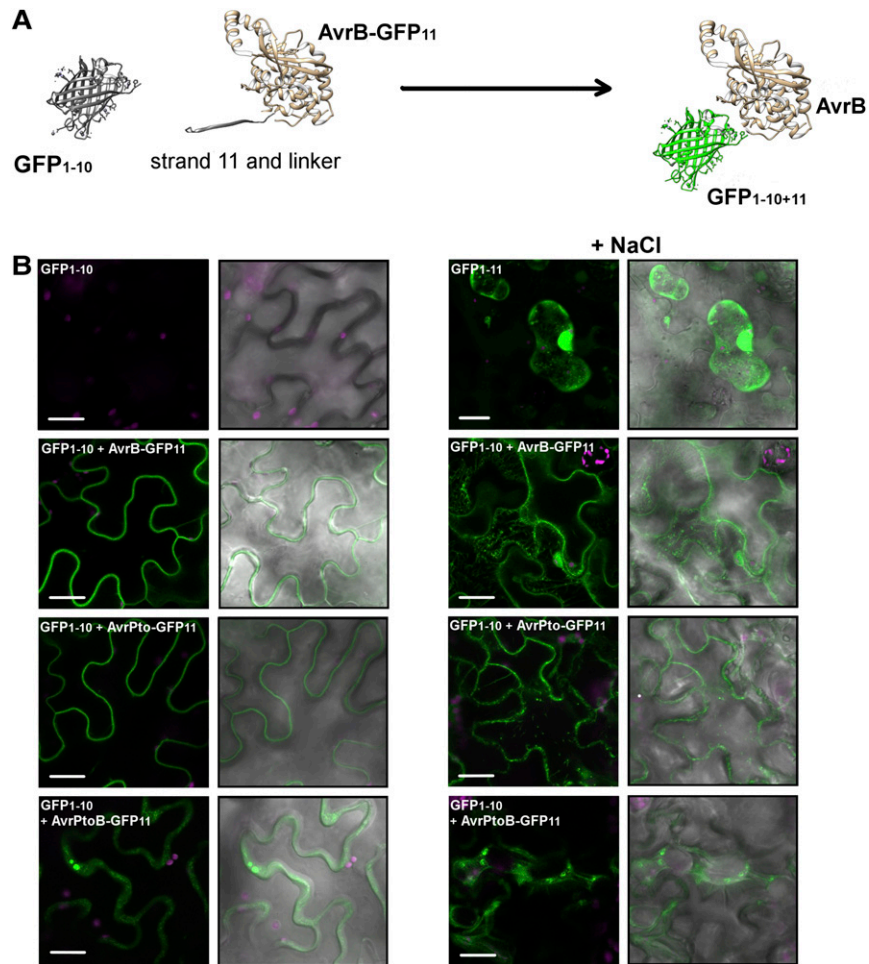


Figure 2. The GFP Strand System Is Able to Detect Effector Localization in *N. benthamiana*.

(A) Overview of the GFP strand system for effector detection in planta. Superfold GFP is a beta barrel protein consisting of 11 strands. GFP can be split into strands 1 to 10, which are transformed into plant cells and constitutively expressed. GFP strand 11 is fused to the C terminus of a bacterial effector via a flexible linker. Here, the AvrB effector is C-terminally tagged with GFP₁₁. When AvrB-GFP₁₁ is expressed in planta, GFP₁₋₁₀ and AvrB-GFP₁₁ spontaneously recombine to give a functional fluorescent GFP molecule. A protein model of super-folder GFP and AvrB was generated from existing crystal structures (PDB: 2B3P and 1NH1, respectively).

(B) Validation of the GFP strand system in *N. benthamiana* using *Agrobacterium*-mediated transient expression of GFP₁₋₁₀ and the *P. syringae* effectors AvrB-GFP₁₁, AvrPto-GFP₁₁, and AvrPtoB-GFP₁₁. GFP fluorescence was visualized by confocal microscopy 48 h postinfiltration. Right panel: Plant leaves were subjected to plasmolysis with 1 M NaCl for 5 min. Plasmolysis demonstrates that the subcellular localization of AvrB and AvrPto effectors are at the plasma membrane and the AvrPtoB effector is cytosolic. GFP₁₋₁₀ alone was used as a negative control and full-length GFP was used as a positive control for plasmolysis. Bar = 20 μm.

AvrPto-GFP₁₁, and AvrPtoB-GFP₁₁ at 24 and 48 hpi. At 24 hpi, effector delivery events were detected in mesophyll cells for AvrB-GFP₁₁ and AvrPto-GFP₁₁ (Supplemental Figure 3; Figure 4D). Delivery events of AvrB-GFP₁₁ and AvrPto-GFP₁₁ effectors at this time point were visualized as small foci at the cell periphery in both mesophyll and epidermal pavement cells (Supplemental Figure 3). At 24 hpi, AvrPtoB-GFP₁₁ was not detected in mesophyll cells, but a small amount of fluorescence was observed in the epidermal pavement cells and the GFP signal had a more diffuse localization around the cell periphery than the other two effectors (Supplemental Figure 3; Figure 4D). By 48 hpi, we observed robust delivery of all three effectors in both mesophyll

and epidermal pavement cells (Figures 4A and 4B). The number of cells positive for GFP fluorescence was greater for the effectors AvrB-GFP₁₁ and AvrPto-GFP₁₁ than for AvrPtoB-GFP₁₁, suggesting enhanced effector delivery or stability (Figure 4D). At 48 hpi, fluorescent stretches of effectors were observed, indicating effector accumulation over time (Figures 4A and 4B). Surprisingly, the highest frequency of delivery events was not in the mesophyll, but the epidermal pavement cells (Figure 4D). GFP fluorescence localized to the cell periphery was observed at both 24 and 48 hpi (Supplemental Figure 3; Figure 4B). The AvrB-GFP₁₁ signal was strongest of the three effectors investigated and was frequently detected at junctions between pavement

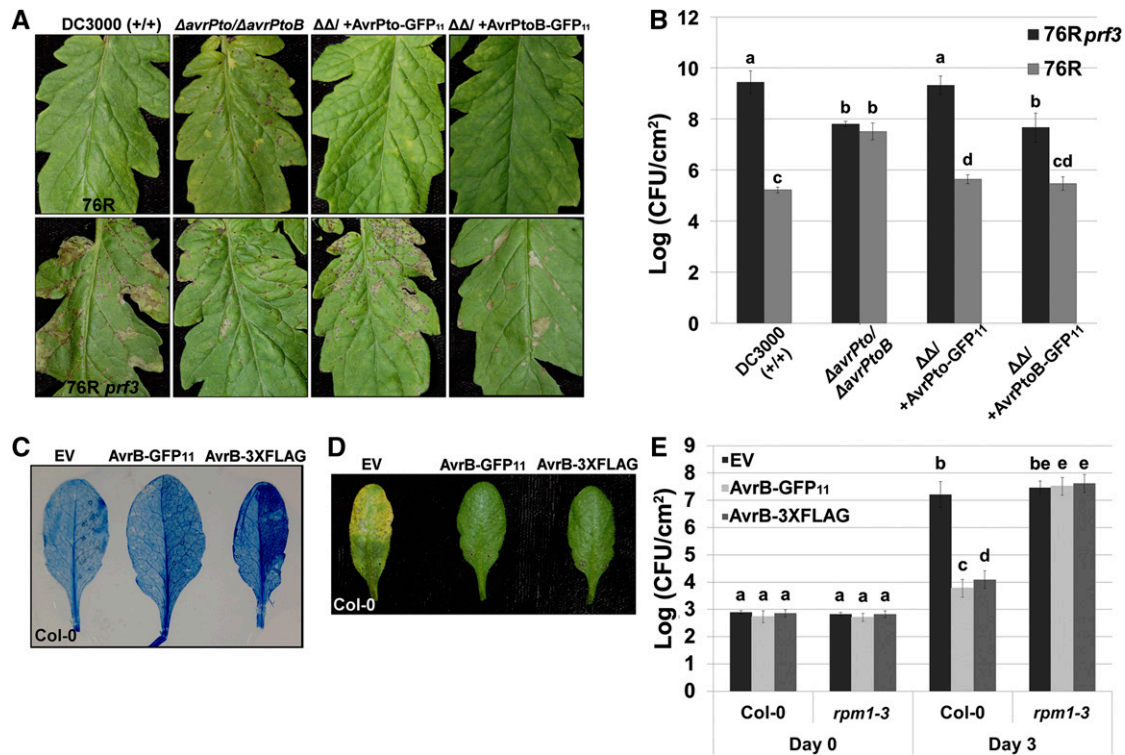


Figure 3. Effectors Fused to GFP₁₁ Retain Their Biological Activity.

Functional validation of strand 11 tagged effectors delivered by *Pst* DC3000 in tomato and Arabidopsis.

(A) Disease symptoms on indicated tomato genotypes 4 d postinoculation. Four-week-old tomato plants were dip inoculated with the indicated strains. Effectors were expressed from their native promoters in the pBBR1 broad host range vector. Tomato RG 76R recognizes the AvrPto and AvrPtoB effectors and is resistant to *Pst* DC3000, but not DC3000 $\Delta\text{avrPto}/\Delta\text{avrPtoB}$ ($\Delta\Delta$). The tomato line RG 76R *prf3* is unable to recognize the AvrPto and AvrPtoB effectors and is susceptible to *Pst* DC3000. RG 76R *prf3* exhibits characteristic necrotic lesions when inoculated with DC3000 (+*avrPto*/+*avrPtoB*), DC3000 $\Delta\Delta$ (+*avrPto*-GFP₁₁), and DC3000 $\Delta\Delta$ (+*avrPtoB*-GFP₁₁).

(B) Quantification of bacterial growth in tomato. Bacterial inoculations were conducted as described in **(A)**, and bacterial titers were determined 4 d postinoculation. RG 76R is able to recognize DC3000 $\Delta\text{avrPto}/\Delta\text{avrPtoB}$ complemented with either AvrPto-GFP₁₁ or AvrPtoB-GFP₁₁. The susceptible cultivar 76R *prf3* cannot mount a response to AvrPto-GFP₁₁ or AvrPtoB-GFP₁₁. Bacterial titers are represented as Log colony-forming units per cm² (Log CFU/cm²) of leaf tissue. Bars represent means, $n = 6$ individual plants, and error bars indicate *sd*. Statistical differences were conducted with by ANOVA followed by LSD mean separation, $\alpha = 0.05$. The experiment was repeated three times with similar results.

(C) The AvrB effector is recognized by the RPM1 immune receptor in Arabidopsis Col-0. DC3000 carrying *avrB*-GFP₁₁ or *avrB*-3xFLAG is recognized in Arabidopsis Col-0 and elicits cell death, as visualized by trypan blue staining. The DC3000 EV control does not elicit cell death. Four-week-old plants were syringe infiltrated in one leaf half with the indicated bacterial genotypes and leaves harvested for trypan blue staining 12 hpi.

(D) Disease symptoms of Arabidopsis Col-0 4 d post-syringe infiltration with DC3000 (EV), *avrB*-GFP₁₁, or *avrB*-3XFLAG.

(E) Quantification of bacterial growth from leaves infiltrated as described in **(D)**. Bacterial titers demonstrate significantly reduced growth of DC3000 (*avrB*-GFP₁₁) compared with DC3000 (EV) on Col-0 but not *rpm1-3*. Bars represent means, $n = 4$ individual plants at day 0, and $n = 8$ individual plants at day 4. Error bars indicate *sd* from the mean. Statistical differences were conducted with by ANOVA followed by LSD mean separation, $\alpha = 0.05$. The experiment was repeated twice with similar results.

cells. Delivery into adjacent pavement cells could be detected as parallel stretches of GFP fluorescence (Figure 4B, inset). To clearly demonstrate separation of the GFP signal and chlorophyll autofluorescence, we used the Zeiss ZEN lite software to create 3D projections of representative Z-stacks for each effector (Figure 4C). These projections further establish a predominance of GFP signal in the epidermal layer. This may reflect a preference for effector delivery at the leaf surface, or it may be a consequence of signal reduction when attempting to move the focal plane more deeply into the leaf interior. Expression of GFP₁₋₁₀ under the control of 35S promoter within individual cell types may

vary and contribute to an observational bias for effector delivery in cells with higher expression of the transgene. We did not detect GFP fluorescence after inoculation with the control *Pst* strains DC3000 EV, DC3000 ΔhrcC carrying effector-GFP₁₁ constructs, or DC3000 $\Delta\text{avrPto}/\Delta\text{avrPtoB}$, indicating that the fluorescence signal was specifically detecting effector delivery (Figures 4A and 4B).

Syringe inoculation delivers bacteria directly to the apoplast. Surface inoculation (dip or spray inoculation) more closely mimics natural infection conditions, enables epiphytic growth on the surface of leaves, and facilitates the detection of early invasion

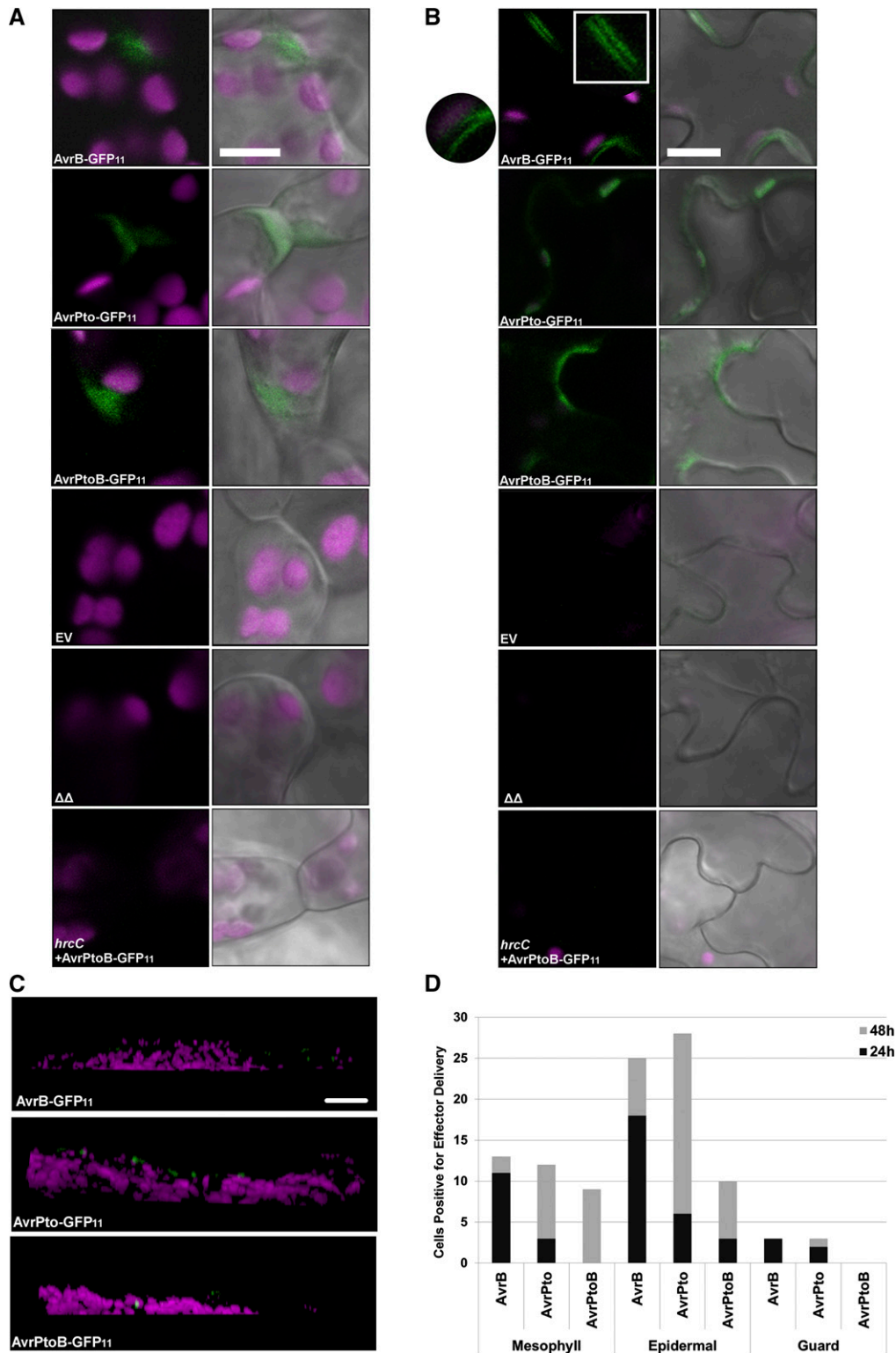


Figure 4. The GFP Strand System Enables Visualization of Type III Delivered Effectors into Diverse Cell Types.

Four-week-old *Arabidopsis* plants expressing 35S:*GFP*₁₋₁₀ were syringe infiltrated with *Pst* DC3000 expressing GFP₁₁-tagged effectors and effector delivery was visualized by confocal microscopy at 24 and 48 hpi.

events into the leaf interior (Katagiri et al., 2002). Due to the robust delivery of AvrB-GFP₁₁ and AvrPto-GFP₁₁ and their plasma membrane localization (effectively concentrating the fluorescent signal), we chose to focus on these two effectors for surface inoculation experiments. In surface-inoculated leaves, effector delivery events were primarily detected in epidermal pavement and guard cells (Figures 5A to 5C). Guard cells can exhibit autofluorescence in their inner walls flanking the stomatal pore. Therefore, guard cells only exhibiting fluorescence in their inner walls were not included in the quantification of effector delivery. Effector delivery was detected when fluorescence occurred at the guard cell outer edge, which is adjacent to the surrounding epidermal pavement cells. Effector delivery into pavement cells gave characteristic stretches of GFP fluorescence at the cell periphery, while delivery events into guard cells appeared as more discretely localized in puncta (Figures 5B). It is possible that effector delivery is initially concentrated as foci at the membrane near the tip of the TTSS needle before spreading along the plasma membrane, as previously described *in vitro* (Jin and He, 2001). Although we were able to visualize AvrB-GFP₁₁ delivered into mesophyll cells at 24 hpi, AvrPto-GFP₁₁ could not be detected in mesophyll cells after surface inoculation at 24 or 48 hpi (Supplemental Figure 4; Figures 5A and 5C). Regardless of the inoculation method, we observed that epidermal pavement cells exhibited the highest number of cells positive for effector delivery (Figures 4C, 5C, and 5D). These data indicate that pavement cells are sites for effector delivery by *P. syringae*. These findings are supported by previously published work, which demonstrated that transcription of *avrPto* in *P. syringae* was highest on the leaf surface when bacteria were in contact with pavement cells (Lee et al., 2012).

Epidermal pavement cells in *Arabidopsis* display a wide size distribution with dimensions ranging 10 to 200 μm , correlated with endopolyploidy of the cell (Melaragno et al., 1993). In contrast, the average size of an epiphytically colonizing *P. syringae* is 1.2 μm (Monier and Lindow, 2003a). The size disparity between bacterial and host cells at the leaf surface could enable multiple bacterial cells to attach and deliver effectors into the same host cell from discrete locations. In order to investigate the ability of *Pst* DC3000 to deliver effectors at multiple sites within each cell, we quantified the number of distinct fluorescent foci within an individual cell from confocal micrographs. The number of fluorescent foci per cell differed depending on the effector and ranged from 1 to 25 (Supplemental Figure 5). Compared with other effectors,

AvrPto-GFP₁₁ exhibited a significantly higher number fluorescent foci in pavement cells at 48 hpi, but a significantly lower number of foci in mesophyll cells at 24 hpi (Supplemental Figure 5). At 24 hpi, AvrB-GFP₁₁ was not only delivered into more mesophyll cells than AvrPto-GFP₁₁, but the number of distinct foci in a single mesophyll cell was also significantly higher (Supplemental Figures 5C and 5D). Taken together, these data demonstrate that the GFP strand system allows analysis of native promoter driven effector delivery during natural infection and the positive detection of cells targeted for effector delivery.

The GFP Strand System Allows Visualization of Effector Delivery by the Xylem Colonizing Pathogen *R. solanacearum*

To demonstrate the utility of the GFP strand system across diverse bacterial pathogens, we applied this technology to detect effector delivery from *R. solanacearum*. This soil-borne Gram-negative bacterial pathogen colonizes the xylem of infected plants, causing devastating bacterial wilt disease in over 200 plant species (Schell, 2000). In contrast to *P. syringae*, *R. solanacearum* gains entry through the root apex or secondary root emergence sites. After invading the root xylem vessels, *R. solanacearum* disseminates into the stem, where it multiplies and induces wilting through excessive production of exopolysaccharides (Schell, 2000). Mutation of core *R. solanacearum* TTSS components renders the bacteria nonpathogenic (Arlat et al., 1992). PopP2 is a well-characterized effector from the *R. solanacearum* strain GMI1000. PopP2 contains a nuclear localization signal and is targeted to the nucleus where it inactivates defensive plant transcription factors to dampen basal immunity (Deslandes et al., 2003). In the *Arabidopsis* Ws-0 ecotype, PopP2 is recognized by the NLR receptors RPS4 and RRS1-R that cooperate molecularly to trigger resistance (Deslandes et al., 2003; Tasset et al., 2010; Le Roux et al., 2015; Sarris et al., 2015).

Using the GFP strand system, we investigated PopP2 delivery during natural infection with *R. solanacearum* GMI1000. PopP2-GFP₁₁ was cloned into the integrative plasmid pRCT under its native promoter and transformed into *R. solanacearum* GMI1000 $\Delta popP2$ (Monteiro et al., 2012). In order to determine if PopP2-GFP₁₁ was functional when delivered from *R. solanacearum*, susceptible *Arabidopsis* Col-0 and resistant Ws-0 plants were root-inoculated (Figure 6A). Compared with the GMI1000 $\Delta popP2 + popP2$, $\Delta popP2$ complemented with *PopP2-GFP₁₁* had similar

Figure 4. (continued).

- (A) Effector delivery into mesophyll cells 48 h post-syringe inoculation. AvrB-GFP₁₁ was visualized after inoculation onto *rpm1-3/rps2-101c (r1r2)* plants expressing GFP₁₋₁₀. AvrPto-GFP₁₁ and AvrPtoB-GFP₁₁ were visualized after inoculation onto Col-0 expressing GFP₁₋₁₀. Effectors were expressed from their native promoters in the broad host range vector pBBR1. EV = pBBR1 empty vector; $\Delta\Delta$ = DC3000 $\Delta avrPto/\Delta avrPtoB$. Bar = 10 μm .
- (B) Effector delivery into the epidermal pavement cells of Col-0 and *r1r2* expressing GFP₁₋₁₀ 48 h post-syringe inoculation. Inset and circle highlight plasma membrane GFP localization in two adjacent epidermal cells for the AvrB-GFP₁₁ effector. Bar = 20 μm .
- (C) Cross-sectional views of syringe inoculated leaves indicate effector delivery predominately localizes to the epidermal cell layers. Each effector cross section represents the time of maximal delivery for that effector; AvrB-GFP₁₁ cross section is from 24 hpi and AvrPto-GFP₁₁ and AvrPtoB-GFP₁₁ cross sections are from 48 hpi. Cross sections were generated from 3D projections of Z-stacks ranging from 15 to 27 μm in thickness. Magenta indicates chlorophyll autofluorescence. Bar = 20 μm .
- (D) Graph indicates the overall temporal differences in delivery of three effectors across cell types in both surface and syringe inoculations, $n = 4$ individual plants per treatment. Numbers reflect the sum of all positive cells over four individual plant replicates at 24 and 48 hpi after both syringe and surface inoculation.

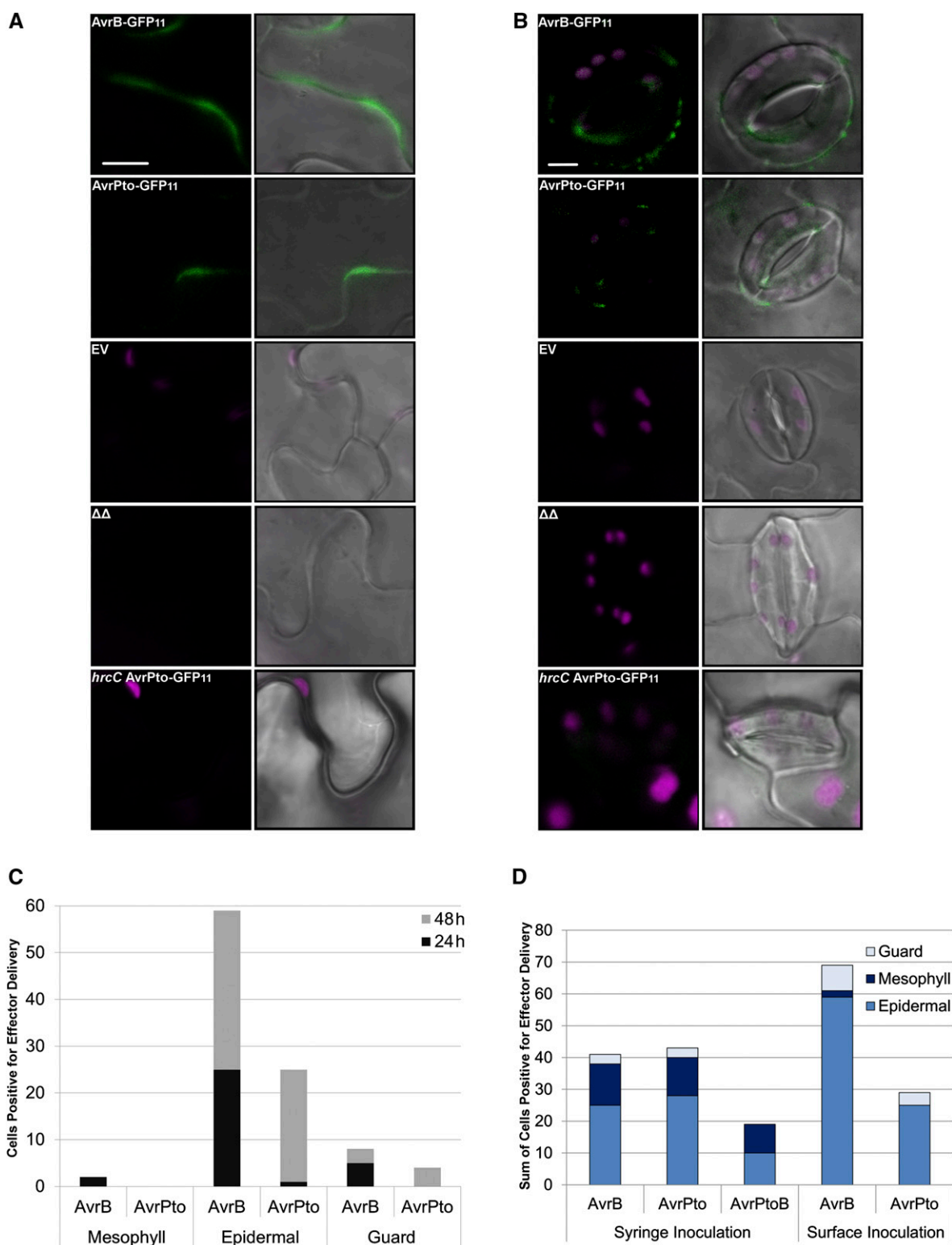


Figure 5. Visualization of DC3000 Type III Delivered Effectors in Arabidopsis after Surface Inoculation.

Two-week-old Arabidopsis plants expressing $35S::GFP_{1-10}$ were painted with *Pst* expressing EV, AvrPto-GFP₁₁, and AvrB-GFP₁₁. Effector delivery was visualized by confocal microscopy 24 and 48 hpi. AvrB-GFP₁₁ was visualized after inoculation onto *rpm1-3/rps2-101c (r1r2)* plants expressing GFP₁₋₁₀.

levels of disease development in Col-0 and the Col-0 *GFP₁₋₁₀* transgenic lines (Figure 6A). Similarly, both strains were recognized in the Ws-0 ecotype. Bacterial virulence of PopP2-containing strains was recovered in the absence of NLR recognition in *rrs1-1* and *rps4-21/rrs1-1* mutant lines (Figure 6A). PopP2 is a member of the YopJ-like family of acetyltransferases and the PopP2-C321A catalytic mutation abolishes effector recognition in Ws-0 (Tasset et al., 2010). The *R. solanacearum* $\Delta popP2+popP2-C321A$ catalytic mutant had a slight reduction in disease severity in susceptible Col-0 and Col-0 35S:*GFP₁₋₁₀* lines compared with PopP2 and PopP2-GFP₁₁, using a previously described disease scale (Figure 6A) (Tasset et al., 2010). These results demonstrate that the PopP2-GFP₁₁ is functionally similar to the wild-type PopP2 in both susceptible and resistant Arabidopsis ecotypes.

To investigate delivery of PopP2-GFP₁₁, 4-week-old Col-0 *GFP₁₋₁₀* plants were root-inoculated with *R. solanacearum* GMI1000 $\Delta popP2+popP2-GFP_{11}$ as previously described (Deslandes et al., 2003) and confocal micrographs were taken 7 d postinoculation. *R. solanacearum* PopP2-GFP₁₁ was observed accumulating in nuclei of cells surrounding the sites of lateral root emergence (Figures 6B to 6D). Roots inoculated with *R. solanacearum* GMI1000 $\Delta popP2+popP2$ did not show fluorescence accumulation in the nuclei (Figures 6E and 6F). Interestingly, PopP2-GFP₁₁ nuclear accumulation was also observed in cells surrounding vasculature in the shoot petiole (Figure 6G). These results demonstrate the functionality and translatability of the GFP strand system for detecting effector delivery across pathogens colonizing diverse host tissues. Effectors delivered to the cytoplasm, plasma membrane, and nucleus can be visualized with the 35S:*GFP₁₋₁₀* system. However, effector visualization is dependent on the subcellular distribution of GFP₁₋₁₀, and it is likely that specific organelle-targeted variants of GFP₁₋₁₀ will be necessary to visualize effector in other cellular organelles.

DISCUSSION

Over 30 effectors are delivered by *P. syringae* DC3000 and over 72 by *R. solanacearum* GMI1000 (Alfano and Collmer, 2004; Coll and Valls, 2013). Pathogen effectors are virulence factors that suppress diverse aspects of plant immunity and thus can be excellent cellular probes for investigating plant innate immune responses (Toruño et al., 2016). Here, we developed the GFP strand system to facilitate investigation of effector delivery and function during natural infection. We demonstrated that four effector-GFP₁₁ fusions are functional, delivered by the TTSS, and

can be visualized in planta using the GFP strand system. Thus, the GFP strand system provides a powerful tool to examine effector biology, including temporal and spatial differences in effector delivery.

P. syringae is a hemibiotrophic pathogen, and it is currently unknown how the switch from biotrophy to necrotrophy is regulated in planta (Xin and He, 2013). Filamentous pathogens demonstrate spatial and temporal regulation of effector expression (Wang et al., 2011; Kleemann et al., 2012). Effector transcription is temporally regulated in filamentous pathogens corresponding to the switch between biotrophic and necrotrophic life stages. In filamentous pathogens, cell death-suppressing effectors are expressed early and cell death-promoting effectors are expressed later during infection (Wang et al., 2011; Kleemann et al., 2012; Jupe et al., 2013). *P. syringae* effectors share a common *hrp* box in their promoter sequences that is recognized by the alternative sigma factor HrpL (Xin and He, 2013). The presence of a conserved *hrp* box indicates that the transcriptional regulation of individual bacterial effectors may not differ. Using the GFP strand system, we detected differences in the quantity of *P. syringae* effector delivery over time. For example, AvrB-GFP₁₁ was most easily detected in planta. Robust AvrB delivery is consistent with the robust activation of RPM1-mediated resistance. RPM1 can trigger a macroscopic HR at 5 to 6 hpi, compared with other NLRs that trigger an HR around 10 to 12 hpi (Boyes et al., 1998). The differences we detected in effector abundance and number of delivery events per cell may reflect kinetics of effector maturation or stability or a difference in substrate preference of the TTSS for different effectors. Additionally, variation in plasmid copy number or replication may have contributed to observed effector delivery differences, although all three *P. syringae* effectors were expressed from the same freely replicating plasmid, pBBR1, which should limit such variation. Future research will focus on investigating effector delivery after integrating the GFP₁₁ tag into endogenous sites at the C termini of effectors in the genome. Our data indicate that variation in effector delivery may exist for *P. syringae* and paves the way for future detailed investigations into the hierarchy of effector delivery using the GFP strand system.

Effector proteins play an important role in epiphytic leaf colonization. Previous studies using *P. syringae* pv *syringae* B728a detected bacterial effector expression at 24 and 48 hpi on the leaf surface, and bacterial strains with mutations in the TTSS exhibited reduced epiphytic growth (Lee et al., 2012). In a natural infection, *P. syringae* initially colonizes the leaf surface, with aggregates forming at cell-cell junctions between pavement cells (Monier and

Figure 5. (continued).

AvrPto-GFP₁₁ was visualized after inoculation onto Col-0 expressing GFP₁₋₁₀. Effectors were expressed from their native promoters in the broad host range vector pBBR1.

- (A) Effector delivery into epidermal pavement cells 48 h post-surface inoculation. EV = pBBR1 empty vector; $\Delta\Delta$ = DC3000 $\Delta avrPto/\Delta avrPtoB$. Bar = 20 μ m.
 (B) Effector delivery into guard cells 48 h post-surface inoculation. Both AvrB-GFP₁₁ and AvrPto-GFP₁₁ were delivered into epidermal guard cells. Bar = 5 μ m.
 (C) Temporal distribution of effector delivery into mesophyll, epidermal pavement, and guard cells differs for each effector. Graph indicates the total number of cells where effector delivery was detected after surface inoculation, $n = 4$ individual plants per treatment and time point. Numbers reflect the sum of all positive cells at 24 or 48 hpi.
 (D) Graph indicates cell-type-specific distribution of effector delivery, contrasting syringe, and surface inoculations, $n = 4$ individual plants per treatment and time point. Numbers reflect the sum of all positive cells at both 24 and 48 hpi.

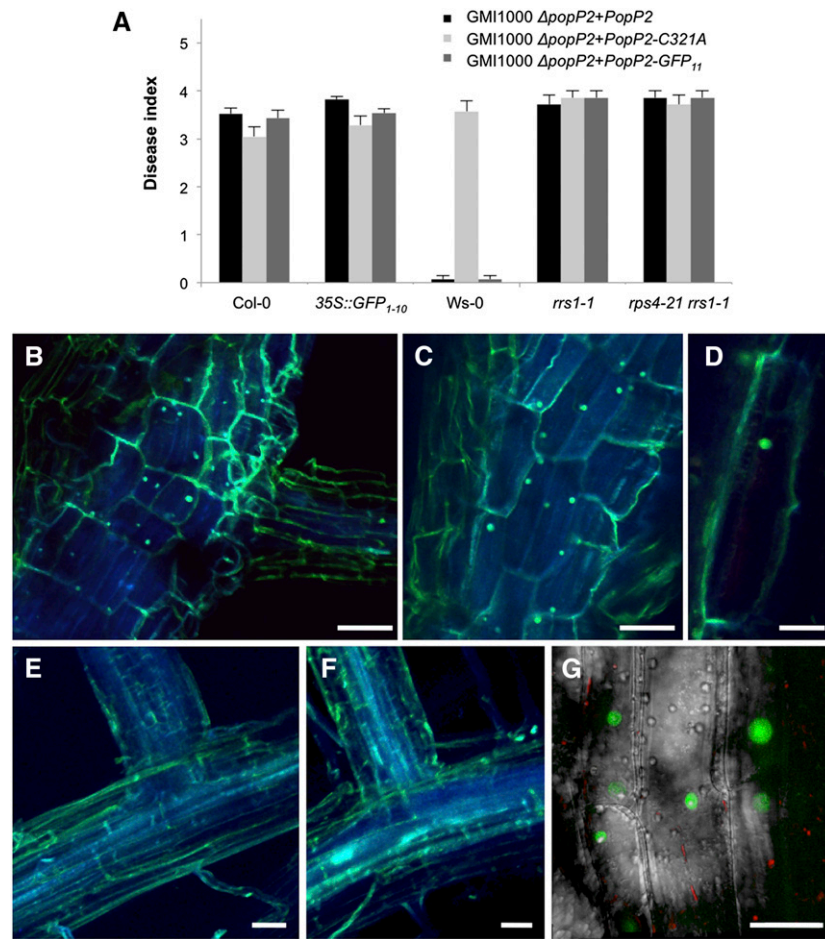


Figure 6. The GFP Strand System Enables Visualization of the *R. solanacearum* PopP2 Effector in the Nuclei of Root and Petiole Cells.

(A) Roots of 4-week-old plants were inoculated with the indicated *R. solanacearum* genotypes, and disease symptoms were scored 8 d postinoculation. The inoculated plant genotypes included Col-0 (does not recognize PopP2), transgenic Col-0 expressing GFP₁₋₁₀, Ws-0 (recognizes PopP2), the *rrs1-1* mutant, and the *rps4-21/rrs1-1* double mutant. Plants were inoculated with *R. solanacearum* GMI1000 $\Delta popP2$ expressing wild-type PopP2, PopP2-C321A, or PopP2-GFP₁₁. The disease index was scored based on the following scale: 0 = no wilting, 1 = 25%, 2 = 50%, 3 = 75%, and 4 = 100% of wilted leaves. Mean and sd values were calculated from scores of >7 plants.

(B) to (D) Confocal micrographs showing the presence of PopP2-GFP₁₁ effector in nuclei of root cells, 7 d postinoculation of 4-week-old transgenic Col-0 35S::GFP₁₋₁₀ plants with *R. solanacearum* GMI1000 $\Delta popP2$ expressing PopP2-GFP₁₁.

(E) and (F) Confocal micrographs of root cells of transgenic Col-0 35S::GFP₁₋₁₀ plants 7 d postinoculation with *R. solanacearum* GMI1000 $\Delta popP2$ expressing PopP2 (negative control). Note no nuclear signal is observed. **(B) and (C)** and **(E) and (F)** are an overlay of maximal projections from 20 to 25 confocal planes acquired in Z-dimension (Z-stacks 4 μ m in thickness). **(D)** is an overlay of a confocal plane.

(G) Confocal images of Col-0 35S::GFP₁₋₁₀ petioles inoculated with *R. solanacearum* GMI1000 $\Delta popP2$ expressing PopP2-GFP₁₁. Bars = 30 μ m.

Lindow, 2003b; Lee et al., 2012). We observed effector delivery at the pavement cell junctions (Figure 4B), supporting cell junctions as important environmental niches for *P. syringae* colonization and initiation points for effector dissemination. Effector delivery into pavement cells occurred after syringe or surface inoculation indicating *P. syringae* can directly deliver diverse effectors into pavement cells on the cell surface or once inside the leaf from the apoplast. Pavement cells have been shown to actively sense pathogen-associated microbial patterns (PAMPs), triggering immune responses such as actin filament rearrangements required for delivery of antimicrobial compounds to infection sites, callose deposition, or mobilization of immune response machinery via the

secretory pathway (Henty-Ridilla et al., 2013). Likewise, *P. syringae* effectors HopW1 and HopG1 have been shown to disrupt actin dynamics to suppress these host cell immune responses (Kang et al., 2014; Shimono et al., 2016). Thus, targeting effector delivery into pavement cells may be an attempt to inhibit or delay plant perception.

Stomatal pores on the leaf surface serve as ports of entry into the leaf interior for multiple pathogens, including *P. syringae* (McLachlan et al., 2014). Several effectors (AvrB, HopX1, HopZ1a, and HopF2) have been shown to interfere with PAMP-induced stomatal closure and promote pathogen entry to the leaf apoplast (Jiang et al., 2013; Gimenez-Ibanez et al., 2014; Hurley et al., 2014;

Zhou et al., 2015). Here, we demonstrated that AvrB and AvrPtoB can be directly delivered into guard cells, which flank stomatal pores, upon surface inoculation using the GFP strand system. Thus, guard cells can be directly targeted by pathogen effectors to promote colonization. Consistent with this finding, AvrB has been demonstrated to promote bacterial growth and stomatal opening upon surface inoculation (Zhou et al., 2015). Collectively, these data indicate that effectors can be directly delivered into cells of the leaf surface in order to enhance entry into the leaf interior and suppress defense responses.

Relatively little is known about the delivery of effectors by vascular pathogens such as *R. solanacearum*. Xylem vessels are non-living water conduits within the plant and are thus poor reservoirs of nutrients to support a pathogenic microbial population (Yadeta and J Thomma, 2013). Effectors from xylem-limited pathogens are thought to be delivered into surrounding live tissues. Multiple NLR immune receptors have been identified recognizing effectors from xylem-colonizing pathogens, including ZAR1 that recognizes AvrAC from *Xanthomonas campestris* and the RRS1-R/RPS4 pair recognizing PopP2 from *R. solanacearum* (Le Roux et al., 2015; Sarris et al., 2015; Wang et al., 2015). Furthermore, the TTSS is absolutely required for the ability of *R. solanacearum* to cause bacterial wilt disease, highlighting the importance of effector delivery (Schell, 2000).

We were able to visualize the *R. solanacearum* effector PopP2-GFP₁₁ at lateral root sites, suggesting effector delivery is important for early colonization. *R. solanacearum* invades plant roots through wounds or cracks, primarily those caused by lateral root emergence (Vasse et al., 1995). Effector delivery at these sites of invasion could be important to suppress early defense responses until *R. solanacearum* can gain entry into the xylem vessels. Once established in the xylem vessels, the bacteria are able to enter the intercellular spaces of the parenchyma cells in the cortex and pith in various areas of the plant (Deslandes et al., 1998). Consistent with this, we were able to detect PopP2-GFP₁₁ delivery and nuclear localization in cells surrounding vasculature. Delivery of effectors from the xylem to surrounding live tissue cells may also metabolically reprogram host cells to support pathogen proliferation.

The GFP strand system is versatile and we have demonstrated its capability to enable visualization of effector delivery in a foliar, epiphytic bacterial pathogen in addition to a root-associated, xylem-colonizing vascular pathogen. This system could be used to investigate effector delivery across kingdoms and may work well for fungal, oomycete, and viral protein delivery. The short GFP strand 11 did not interfere with effector function, as opposed to a full-length fluorophore that would not be delivered by the TTSS and can also interfere with effector function in planta (Akeda and Galán, 2005; Van Engelenburg and Palmer, 2010; Radics et al., 2014). Natural infection allows visualization of effector localization within host cells. For example, we observed discrete fluorescent puncta or short fluorescent stretches at the cell periphery for AvrB-GFP₁₁ and AvrPto-GFP₁₁ in inoculated leaves, indicating effectors are delivered in nonhomogenous microenvironments within a cell (Figures 4 and 5; Supplemental Figures 3 and 4). This is in contrast to robust fluorescence observed around the entire cell periphery in our transient overexpression validation assays for the GFP strand system in *N. benthamiana* (Figure 2). Creation of microenvironments within a host cell by delivering effectors into discrete

subcellular locations may play a key role in effector function during natural infection. Taken together, the GFP strand system provides effector biologists in with a valuable tool to advance the understanding plant-pathogen interactions.

METHODS

Plant Materials and Growth Conditions

Arabidopsis thaliana plants were grown in a controlled environment chamber at 23°C, 75% relative humidity, and a 10-h/14-h light/dark photoperiod with light intensity of 100 $\mu\text{E m}^{-2} \text{s}^{-1}$ using T12 high output bulbs. The *rps2-101c/rpm1-3* and *rps2-101c/rpm1-3/rin4* genotypes were previously described (Mindrinos et al., 1994; Boyes et al., 1998; Mackey et al., 2002). Line *r2* refers to *rps2-101c*, *r1* refers to *rpm1-3*, and *r4* refers to *rin4* (Mindrinos et al., 1994; Boyes et al., 1998). Seedlings used in detecting GFP₁₋₁₀ expression in roots versus shoots were grown on Murashige and Skoog plates for 2 weeks before harvesting. *Nicotiana benthamiana* plants were grown in a controlled environmental chamber at 25°C, 85% relative humidity, and 16/8-h light/dark photoperiod with light intensity of 180 $\mu\text{E m}^{-2} \text{s}^{-1}$. Tomato (*Solanum lycopersicum* cv Rio-Grande) 76R lines [RG (*Pto/Pto*, *Prf/Prf*), RG *prf3* (*Pto/Pto*, *prf3/prf3*)] were grown as previously described (Thapa et al., 2015).

Molecular Cloning

All primers used for cloning are described in Supplemental Table 1. The cell-specific promoters pGC1 (Yang et al., 2008; 1730 bp), pCER6 (Ranjan et al., 2011; 1230 bp), and pCAB3 (Ranjan et al., 2011; 1550 bp) were PCR amplified and cloned into pENTR (Invitrogen). *RIN4*'s genomic DNA with an N-terminal fusion to the T7 epitope was cloned into pENTR as previously described (Lee et al., 2015). Cell-specific promoter T7-gRIN4 constructs were moved into the binary vector pGWB1 using Gateway technology (Invitrogen; Nakagawa et al., 2007). The *Arabidopsis rps2-101c/rin4* mutant was used as the background genotype for all cell-specific promoter transformations. All transgenic plants were generated using the floral-dip method and homozygous T3 lines were used for all assays (Clough and Bent, 1998). For effector delivery assays, *Arabidopsis Col-0* and *rpm1-3/rps2-101C (r1r2)* backgrounds were transformed with pZP222 carrying 35S:GFP₁₋₁₀ by the floral dip method (Clough and Bent, 1998) to generate transgenic plants with constitutive expression of GFP strands 1 to 10.

Bacterial effectors with C-terminal fusions to GFP strand 11 (GFP₁₁) were cloned into binary vectors for expression in *N. benthamiana* as well as broad host range vectors for expression in *Pseudomonas syringae* pv *tomato* (*Pst*) strain DC3000. In-fusion cloning (Clontech) was used to seamlessly clone effector-GFP₁₁ constructs into pGWB514 (Nakagawa et al., 2007), followed by electroporation into *Agrobacterium tumefaciens* strain GV3101 for transient coexpression with 35S:GFP₁₋₁₀. The broad host range vector pBBR1 MCS5 (Kovach et al., 1995) was linearized with *Xho*I and the Gateway cassette B with C-terminal GFP₁₁ was ligated back in, creating a new vector named pBBR1_{GW}-GFP₁₁. The *avrPtoB* promoter and coding sequence was PCR amplified from *Pst*, cloned into pENTR, and moved into pBBR1_{GW}-GFP₁₁. In-fusion cloning (Clontech) was used to seamlessly clone *npro:avrB-GFP₁₁* and *npro:avrPto-GFP₁₁* into pBBR1-MCS5 without the gateway footprint (*npro:avrB* in pBBR1_{GW}-GFP₁₁ was nonfunctional in planta). The pBBR1 *avrPto-GFP₁₁* plasmid and pBBR1_{GW} *avrPtoB-GFP₁₁* plasmid were conjugated into *Pto* DC3000 Δ *avrPto/avrPtoB* using triparental mating (Lin and Martin, 2005). pBBR1_{GW} *avrPtoB-GFP₁₁* was electroporated into *Pst* DC3000 Δ *hrcC* as a negative control for type three secretion of GFP₁₁-tagged effector. The *avrB* promoter and coding sequence was PCR amplified from a previously described pENTR plasmid (Lee et al., 2015). The pBBR1 *avrB-GFP₁₁* plasmid was electroporated into *Pst* DC3000. Native promoters for each effector

were defined as follows: 85 bp upstream ATG for AvrPtoB, 256 bp upstream ATG for AvrB, and 116 bp upstream of ATG for AvrPto. Promoters were designed to include *Hrp* box and intergenic regions.

The PopP2-GFP₁₁ sequence was generated by two-step PCR using PrimeStar HS DNA polymerase from Takara Bio. Primers used are listed in Supplemental Table 1: Fragment 1 was generated using primers PopP2-Fw and PopP2-GFP11-rev, and fragment 2 used primers PopP2-GFP11-Fw and GFP11-Rev. PCR fragment 3, generated by mixing fragments 1 and 2 in presence of primers AttB1-PopP2 and AttB2-GFP₁₁, was recombined into pDONR207 (Invitrogen) to generate the pENTR-PopP2-GFP₁₁ entry clone. The PopP2-GFP₁₁ insert was recombined into the pRCT-GWY destination vector allowing the expression of *PopP2* under the control of its native promoter (383 bp upstream ATG). Integrative pRCT-PopP2-GFP₁₁ plasmid allowing expression of the PopP2-GFP₁₁ coding sequence under the control of native *popP2* promoter was introduced in *Ralstonia solanacearum* GMI1000 $\Delta popP2$ strain by natural transformation.

Immunoblotting

SDS-PAGE and subsequent immunoblotting were performed according to standard procedures (Harlow and Lane, 1988). RIN4 immunoblots were performed with anti-RIN4 rabbit polyclonal antibody at a concentration of 1:3000 (Lee et al., 2015). GFP immunoblots were performed with anti-GFP (ab290; Abcam) rabbit polyclonal antibody at a concentration of 1:8000. Secondary goat anti-rabbit IgG-HRP conjugate (Bio-Rad) was used at a concentration of 1:3000 for detection via enhanced chemiluminescence (Pierce).

Pathogen Assays

Microscopic cell death assays were performed 12 hpi with *Pst* DC3000 (*avrB*). Four-week-old Col-0, pGC1, and pCER6 promoter lines were dip inoculated with 1×10^9 colony-forming units (CFU)/mL, whereas pCAB3 lines were syringe inoculated with 5×10^5 CFU/mL *Pst* DC3000 (*avrB*). Dead cells were visualized using trypan blue staining (9.3 mL phenol [liquid], 10 mL lactic acid, 10 mL glycerol, 10 mL water, and 10 mg trypan blue). Leaves were covered with trypan blue stain (Alfa Aesar) and incubated in a boiling water bath for 5 to 10 min. Samples were allowed to cool at room temp for 45 to 60 min before removing the trypan blue stain and washing three times with water to remove excess stain. Tissue was cleared in chloral hydrate overnight (2.5 g chloral hydrate/mL of water), then transferred to 60% glycerol for storage and microscopy.

For macroscopic cell death assays, *Pst* DC3000 carrying empty pBBR1 and *Pst* DC3000 (*avrB-GFP₁₁* in pBBR1) were syringe infiltrated into 4-week-old Arabidopsis Col-0 leaves at a concentration of 4×10^7 CFU/mL. After infiltration, plants were placed under a light bank and macroscopic cell death (HR) was observed using trypan blue staining at 12 hpi as described above. For the ion leakage assay, leaf disks of infiltrated leaves were harvested with a cork borer #4 and incubated in water for 30 min. Water was replaced and conductivity was measured 5 h later using an Orion 3 Star conductivity meter (Thermo Electron).

Bacterial growth assays in Arabidopsis were performed using syringe inoculation, whereby 4-week-old Col-0 plants were syringe infiltrated with 2×10^5 CFU/mL bacteria in 10 mM MgCl₂ as described by Kim et al. (2005). Experiments were repeated at least twice, with a minimum of six biological replicates (six individual plants) per time point. Bacterial growth assays were performed on 3-week-old tomato plants. The *S. lycopersicum* genotypes Rio Grande 76R (*Pto/Pto*, *Prf/Prf*) and RG *prf3* (*Pto/Pto*, *prf3/prf3*) were dip inoculated with 5×10^7 CFU/mL bacteria in 10 mM MgCl₂ with 0.01% Silwet L-77 as previously described (Thapa et al., 2015). For inoculations with *R. solanacearum* GMI1000 $\Delta popP2$ strains, 4-week-old plants were root inoculated as described before and disease symptoms were scored 7 to 8 d postinoculation (Deslandes et al., 1998).

Microscopy

All microscopy for single-cell HR trypan blue staining was performed using a Leica DM 5000B epifluorescent microscope under bright-field conditions. All confocal microscopy with *P. syringae* infections were performed using a Zeiss LSM710 confocal microscope equipped with a LDC-apochromat40 \times /1.1W KorrM27 water-immersion objective (NA 1.1). GFP was excited at 488 nm, and emission was gathered at 500 to 550 nm. Chloroplast autofluorescence emission was gathered at 650 to 750 nm. Imaging of transient coexpression of effector-GFP₁₁ and GFP₁₋₁₀ in *N. benthamiana* was performed at 36 hpi. *Agrobacterium* strains (described above) carrying 35S:*GFP₁₋₁₀* or *avrPto-GFP₁₁*, *avrPtoB-GFP₁₁* and *avrB-GFP₁₁* were induced with 100 μ M acetosyringone and coinfiltrated at an OD₆₀₀ = 0.6 into *N. benthamiana*. Plasmolysis was performed using 1 M NaCl.

For effector delivery experiments where surface inoculation was used, 2-week-old seedlings of Arabidopsis Col-0, Col-0 *GFP₁₋₁₀*, or *r1r2 GFP₁₋₁₀* were painted with 1×10^9 CFU/mL bacteria resuspended in 10 mM MgCl₂. Effector delivery assays using syringe inoculation were performed on 4-week-old plants using bacterial suspensions of 2×10^6 CFU/mL. The following bacterial strains were used: *Pst* DC3000, *Pst* DC3000 ($\Delta avrPto/\Delta avrPtoB$), *Pst* DC3000 ($\Delta avrPto/\Delta avrPtoB + avrPtoB-GFP₁₁$), *Pst* DC3000 ($\Delta avrPto/\Delta avrPtoB + avrPto-GFP₁₁$), *Pst* DC3000 ($+avrB-GFP₁₁$), *Pst* DC3000 ($\Delta hrnC + avrPtoB-GFP₁₁$), and *Pst* DC3000 ($\Delta hrnC + avrPto-GFP₁₁$). Plant leaves were scanned for the presence of GFP fluorescence to detect effector delivery. Confocal micrographs were collected 24 and 48 hpi. Micrographs taken from four independent plants per treatment were analyzed for delivery into specific cells and discrete delivery events ranging from puncta to larger plasma membrane or cytosolic sheets. A total of 107 micrographs were analyzed, with 63 from the three combined effector treatments. Of the 63 micrographs, 26 were of *Pst* DC3000 ($+avrB-GFP₁₁$), 27 of *Pst* DC3000 ($\Delta avrPto/\Delta avrPtoB + avrPto-GFP₁₁$), and 10 were from *Pst* DC3000 ($\Delta avrPto/\Delta avrPtoB + avrPtoB-GFP₁₁$) inoculated leaves. *Pst* DC3000 ($\Delta avrPto/\Delta avrPtoB + avrPtoB-GFP₁₁$) had fewer total micrographs because it was only tested using syringe inoculation.

Detection of PopP2-GFP₁₁ in root or petiole cells was performed seven days after inoculation of 4-week-old Arabidopsis 35S:*GFP₁₋₁₀* plants with *R. solanacearum* GMI1000 $\Delta popP2$ expressing PopP2-GFP₁₁ or PopP2 (negative control). Entire roots were washed with distilled water, mounted on a glass slide, and covered with a cover slip. Plant petioles and roots were scanned for the presence of GFP fluorescence to detect effector delivery. Images were acquired with a confocal microscope (Leica SP2 AOBs) using a 40 \times water immersion lens (NA 0.8). For excitation, a 405-nm ray line of a diode laser and the 488-nm ray line of an argon laser were used and the emitted fluorescence collected in the blue range between 410 and 470 nm and in the green range between 500 and 530 nm. Maximal projections of 20 to 25 confocal planes were acquired in Z-dimension. From the Z-stack of confocal images, the maximal projections of the two color channels were then computed and overlaid.

Accession Numbers

Sequence data from this article can be found in the Arabidopsis Genome Initiative or GenBank/EMBL databases under the following accession numbers: GC1 (At1g22690), CER6 (At1g68530), CAB3 (At1g29910), RIN4 (At3g25070), RPM1 (At3g07040), RPS2 (At4g26090), PTO (101268866), PRF (101263413), AvrPto (1185679), AvrPtoB (1184744), AvrB (3366713), and PopP2 (16105295).

Supplemental Data

Supplemental Figure 1. RIN4 expression in Arabidopsis tissue-specific lines.

Supplemental Figure 2. GFP₁₋₁₀ is detected by immunoblot using anti-GFP after expression in Arabidopsis and *Nicotiana benthamiana*.

Supplemental Figure 3. Visualization of *Pseudomonas syringae* DC3000 effector delivery in Arabidopsis 24 h post-syringe inoculation.

Supplemental Figure 4. Visualization of *Pseudomonas syringae* DC3000 effector delivery in Arabidopsis 24 h post-surface inoculation.

Supplemental Figure 5. Bacterial effectors are delivered at multiple foci per cell.

Supplemental Table 1. Primers used in experiments listed 5'-3'.

Supplemental Table 2. Analysis of variance of conductivity in Arabidopsis cell-specific promoter lines.

Supplemental Table 3. Analysis of variance of bacterial growth in tomato.

Supplemental Table 4. Analysis of variance of bacterial growth in Arabidopsis.

ACKNOWLEDGMENTS

E.H. was supported by a USDA National Institute of Food and Agriculture predoctoral fellowship (2014-67011-21563). T.Y.T. and G.C. were supported by a National Institutes of Health grant (RO1GM092772) awarded to G.C.L.D. was supported by an ANR grant (RADAR, ANR-15-CE20-0016-01) and the Laboratoire d'Excellence (LABEX) TULIP (ANR-10-LABX-41). A.J. and the TRI-Genotoul platform were supported by the région Occitanie/Pyrénées-Méditerranée (PRISM-Project).

AUTHOR CONTRIBUTIONS

E.H., T.Y.T., L.D., and G.C. designed experiments. E.H., T.Y.T., and A.J. performed experiments. G.C. and L.D. supervised the study. E.H., T.Y.T., and G.C. wrote the manuscript with input from A.J. and L.D.

Received January 12, 2017; revised May 22, 2017; accepted June 8, 2017; published June 9, 2017.

REFERENCES

- Akeda, Y., and Galán, J.E.** (2005). Chaperone release and unfolding of substrates in type III secretion. *Nature* **437**: 911–915.
- Alfano, J.R., and Collmer, A.** (2004). Type III secretion system effector proteins: double agents in bacterial disease and plant defense. *Annu. Rev. Phytopathol.* **42**: 385–414.
- Allan, A.C., and Fluhr, R.** (1997). Two distinct sources of elicited reactive oxygen species in tobacco epidermal cells. *Plant Cell* **9**: 1559–1572.
- Arlat, M., Gough, C.L., Zischek, C., Barberis, P.A., Trigalet, A., and Boucher, C.A.** (1992). Transcriptional organization and expression of the large hrp gene cluster of *Pseudomonas solanacearum*. *Mol. Plant Microbe Interact.* **5**: 187–193.
- Axtell, M.J., and Staskawicz, B.J.** (2003). Initiation of RPS2-specified disease resistance in Arabidopsis is coupled to the AvrRpt2-directed elimination of RIN4. *Cell* **112**: 369–377.
- Boyes, D.C., Nam, J., and Dangl, J.L.** (1998). The Arabidopsis thaliana RPM1 disease resistance gene product is a peripheral plasma membrane protein that is degraded coincident with the hypersensitive response. *Proc. Natl. Acad. Sci. USA* **95**: 15849–15854.
- Cabantous, S., Terwilliger, T.C., and Waldo, G.S.** (2005). Protein tagging and detection with engineered self-assembling fragments of green fluorescent protein. *Nat. Biotechnol.* **23**: 102–107.
- Chang, J.H., Desveaux, D., and Creason, A.L.** (2014). The ABCs and 123s of bacterial secretion systems in plant pathogenesis. *Annu. Rev. Phytopathol.* **52**: 317–345.
- Chiang, Y.-H., and Coaker, G.** (2015). Effector triggered immunity: NLR immune perception and downstream defense responses. *The Arabidopsis Book* **13**: e0183, doi/10.1199/tab.0183.
- Chung, E.H., da Cunha, L., Wu, A.J., Gao, Z., Cherkis, K., Afzal, A.J., Mackey, D., and Dangl, J.L.** (2011). Specific threonine phosphorylation of a host target by two unrelated type III effectors activates a host innate immune receptor in plants. *Cell Host Microbe* **9**: 125–136.
- Clough, S.J., and Bent, A.F.** (1998). Floral dip: a simplified method for Agrobacterium-mediated transformation of *Arabidopsis thaliana*. *Plant J.* **16**: 735–743.
- Coll, N.S., and Valls, M.** (2013). Current knowledge on the *Ralstonia solanacearum* type III secretion system. *Microb. Biotechnol.* **6**: 614–620.
- Deng, W.L., Preston, G., Collmer, A., Chang, C.J., and Huang, H.C.** (1998). Characterization of the hrpC and hrpRS operons of *Pseudomonas syringae* pathovars syringae, tomato, and glycinea and analysis of the ability of hrpF, hrpG, hrpC, hrpT, and hrpV mutants to elicit the hypersensitive response and disease in plants. *J. Bacteriol.* **180**: 4523–4531.
- Deslandes, L., Olivier, J., Peeters, N., Feng, D.X., Khounlotham, M., Boucher, C., Somssich, I., Genin, S., and Marco, Y.** (2003). Physical interaction between RRS1-R, a protein conferring resistance to bacterial wilt, and PopP2, a type III effector targeted to the plant nucleus. *Proc. Natl. Acad. Sci. USA* **100**: 8024–8029.
- Deslandes, L., Pileur, F., Liaubet, L., Camut, S., Can, C., Williams, K., Holub, E., Beynon, J., Arlat, M., and Marco, Y.** (1998). Genetic characterization of RRS1, a recessive locus in Arabidopsis thaliana that confers resistance to the bacterial soil-borne pathogen *Ralstonia solanacearum*. *Mol. Plant Microbe Interact.* **11**: 659–667.
- de Vries, J.S., Andriotis, V.M., Wu, A.J., and Rathjen, J.P.** (2006). Tomato Pto encodes a functional N-myristoylation motif that is required for signal transduction in *Nicotiana benthamiana*. *Plant J.* **45**: 31–45.
- Gimenez-Ibanez, S., Boter, M., Fernández-Barbero, G., Chini, A., Rathjen, J.P., and Solano, R.** (2014). The bacterial effector HopX1 targets JAZ transcriptional repressors to activate jasmonate signaling and promote infection in Arabidopsis. *PLoS Biol.* **12**: e1001792.
- Greenberg, J.T., and Yao, N.** (2004). The role and regulation of programmed cell death in plant-pathogen interactions. *Cell. Microbiol.* **6**: 201–211.
- Harlow, E., and Lane, D.P.** (1988). *Antibodies: A Laboratory Manual.* (Cold Spring Harbor, NY: Cold Spring Harbor Laboratory Press).
- Henry, E., Yadeta, K.A., and Coaker, G.** (2013). Recognition of bacterial plant pathogens: local, systemic and transgenerational immunity. *New Phytol.* **199**: 908–915.
- Henry, E., Fung, N., Liu, J., Drakakaki, G., and Coaker, G.** (2015). Beyond glycolysis: GAPDHs are multi-functional enzymes involved in regulation of ROS, autophagy, and plant immune responses. *PLoS Genet.* **11**: e1005199.
- Henty-Ridilla, J.L., Shimono, M., Li, J., Chang, J.H., Day, B., and Staiger, C.J.** (2013). The plant actin cytoskeleton responds to signals from microbe-associated molecular patterns. *PLoS Pathog.* **9**: e1003290.
- Hurley, B., Lee, D., Mott, A., Wilton, M., Liu, J., Liu, Y.C., Angers, S., Coaker, G., Guttman, D.S., and Desveaux, D.** (2014). The *Pseudomonas syringae* type III effector HopF2 suppresses Arabidopsis stomatal immunity. *PLoS One* **9**: e114921.

- Jiang, S., Yao, J., Ma, K.W., Zhou, H., Song, J., He, S.Y., and Ma, W. (2013). Bacterial effector activates jasmonate signaling by directly targeting JAZ transcriptional repressors. *PLoS Pathog.* **9**: e1003715.
- Jin, Q., and He, S.Y. (2001). Role of the Hrp pilus in type III protein secretion in *Pseudomonas syringae*. *Science* **294**: 2556–2558.
- Jupe, J., Stam, R., Howden, A.J., Morris, J.A., Zhang, R., Hedley, P.E., and Huitema, E. (2013). *Phytophthora capsici*-tomato interaction features dramatic shifts in gene expression associated with a hemi-biotrophic lifestyle. *Genome Biol.* **14**: R63.
- Kang, Y., Jelenska, J., Cecchini, N.M., Li, Y., Lee, M.W., Kovar, D.R., and Greenberg, J.T. (2014). HopW1 from *Pseudomonas syringae* disrupts the actin cytoskeleton to promote virulence in Arabidopsis. *PLoS Pathog.* **10**: e1004232.
- Katagiri, F., Thilmony, R., and He, S.Y. (2002). The Arabidopsis thaliana-*Pseudomonas syringae* interaction. *The Arabidopsis Book* **1**: e0039, doi/10.1199/tab.0039.
- Khang, C.H., Berruyer, R., Giraldo, M.C., Kankanala, P., Park, S.Y., Czymbek, K., Kang, S., and Valent, B. (2010). Translocation of *Magnaporthe oryzae* effectors into rice cells and their subsequent cell-to-cell movement. *Plant Cell* **22**: 1388–1403.
- Kim, M.G., da Cunha, L., McFall, A.J., Belkhadir, Y., DebRoy, S., Dangl, J.L., and Mackey, D. (2005). Two *Pseudomonas syringae* type III effectors inhibit RIN4-regulated basal defense in Arabidopsis. *Cell* **121**: 749–759.
- Kleemann, J., Rincon-Rivera, L.J., Takahara, H., Neumann, U., Ver Loren van Themaat, E., van der Does, H.C., Hacquard, S., Stüber, K., Will, I., Schmalenbach, W., Schmelzer, E., and O'Connell, R.J. (2012). Sequential delivery of host-induced virulence effectors by appressoria and intracellular hyphae of the phytopathogen *Colletotrichum higginsianum*. *PLoS Pathog.* **8**: e1002643.
- Kovach, M.E., Elzer, P.H., Hill, D.S., Robertson, G.T., Farris, M.A., Roop II, R.M., and Peterson, K.M. (1995). Four new derivatives of the broad-host-range cloning vector pBBR1MCS, carrying different antibiotic-resistance cassettes. *Gene* **166**: 175–176.
- Lee, D., Bourdais, G., Yu, G., Robatzek, S., and Coaker, G. (2015). Phosphorylation of the plant immune regulator RPM1-INTERACTING PROTEIN4 enhances plant plasma membrane H⁺-ATPase activity and inhibits flagellin-triggered immune responses in Arabidopsis. *Plant Cell* **27**: 2042–2056.
- Lee, J., Teitzel, G.M., Munkvold, K., del Pozo, O., Martin, G.B., Michelmore, R.W., and Greenberg, J.T. (2012). Type III secretion and effectors shape the survival and growth pattern of *Pseudomonas syringae* on leaf surfaces. *Plant Physiol.* **158**: 1803–1818.
- Le Roux, C., et al. (2015). A receptor pair with an integrated decoy converts pathogen disabling of transcription factors to immunity. *Cell* **161**: 1074–1088.
- Li, X., and Pan, S.Q. (2017). *Agrobacterium* delivers VirE2 protein into host cells via clathrin-mediated endocytosis. *Sci. Adv.* **3**: e1601528.
- Li, X., Yang, Q., Tu, H., Lim, Z., and Pan, S.Q. (2014). Direct visualization of *Agrobacterium*-delivered VirE2 in recipient cells. *Plant J.* **77**: 487–495.
- Lin, N.C., and Martin, G.B. (2005). An avrPto/avrPtoB mutant of *Pseudomonas syringae* pv. tomato DC3000 does not elicit Pto-mediated resistance and is less virulent on tomato. *Mol. Plant Microbe Interact.* **18**: 43–51.
- Liu, J., Elmore, J.M., Lin, Z.J., and Coaker, G. (2011). A receptor-like cytoplasmic kinase phosphorylates the host target RIN4, leading to the activation of a plant innate immune receptor. *Cell Host Microbe* **9**: 137–146.
- Mackey, D., Holt III, B.F., Wiig, A., and Dangl, J.L. (2002). RIN4 interacts with *Pseudomonas syringae* type III effector molecules and is required for RPM1-mediated resistance in Arabidopsis. *Cell* **108**: 743–754.
- Mackey, D., Belkhadir, Y., Alonso, J.M., Ecker, J.R., and Dangl, J.L. (2003). Arabidopsis RIN4 is a target of the type III virulence effector AvrRpt2 and modulates RPS2-mediated resistance. *Cell* **112**: 379–389.
- Martin, G.B., Brommonschenkel, S.H., Chunwongse, J., Frary, A., Ganai, M.W., Spivey, R., Wu, T., Earle, E.D., and Tanksley, S.D. (1993). Map-based cloning of a protein kinase gene conferring disease resistance in tomato. *Science* **262**: 1432–1436.
- McLachlan, D.H., Kopschke, M., and Robatzek, S. (2014). Gate control: guard cell regulation by microbial stress. *New Phytol.* **203**: 1049–1063.
- Melaragno, J.E., Mehrotra, B., and Coleman, A.W. (1993). Relationship between endopolyploidy and cell size in epidermal tissue of Arabidopsis. *Plant Cell* **5**: 1661–1668.
- Mindrinos, M., Katagiri, F., Yu, G.L., and Ausubel, F.M. (1994). The *A. thaliana* disease resistance gene RPS2 encodes a protein containing a nucleotide-binding site and leucine-rich repeats. *Cell* **78**: 1089–1099.
- Monier, J.M., and Lindow, S.E. (2003a). *Pseudomonas syringae* responds to the environment on leaves by cell size reduction. *Phytopathology* **93**: 1209–1216.
- Monier, J.M., and Lindow, S.E. (2003b). Differential survival of solitary and aggregated bacterial cells promotes aggregate formation on leaf surfaces. *Proc. Natl. Acad. Sci. USA* **100**: 15977–15982.
- Monteiro, F., Solé, M., van Dijk, I., and Valls, M. (2012). A chromosomal insertion toolbox for promoter probing, mutant complementation, and pathogenicity studies in *Ralstonia solanacearum*. *Mol. Plant Microbe Interact.* **25**: 557–568.
- Nakagawa, T., Kurose, T., Hino, T., Tanaka, K., Kawamukai, M., Niwa, Y., Toyooka, K., Matsuoka, K., Jinbo, T., and Kimura, T. (2007). Development of series of gateway binary vectors, pGWBs, for realizing efficient construction of fusion genes for plant transformation. *J. Biosci. Bioeng.* **104**: 34–41.
- Nimchuk, Z., Marois, E., Kjemtrup, S., Leister, R.T., Katagiri, F., and Dangl, J.L. (2000). Eukaryotic fatty acylation drives plasma membrane targeting and enhances function of several type III effector proteins from *Pseudomonas syringae*. *Cell* **101**: 353–363.
- Pédélecq, J.D., Cabantous, S., Tran, T., Terwilliger, T.C., and Waldo, G.S. (2006). Engineering and characterization of a superfolder green fluorescent protein. *Nat. Biotechnol.* **24**: 79–88.
- Radics, J., Königsmaier, L., and Marlovits, T.C. (2014). Structure of a pathogenic type 3 secretion system in action. *Nat. Struct. Mol. Biol.* **21**: 82–87.
- Ranjan, A., Fiene, G., Fackendahl, P., and Hoecker, U. (2011). The Arabidopsis repressor of light signaling SPA1 acts in the phloem to regulate seedling de-etiolation, leaf expansion and flowering time. *Development* **138**: 1851–1862.
- Salmeron, J.M., Oldroyd, G.E., Rommens, C.M., Scofield, S.R., Kim, H.S., Lavelle, D.T., Dahlbeck, D., and Staskawicz, B.J. (1996). Tomato Prf is a member of the leucine-rich repeat class of plant disease resistance genes and lies embedded within the Pto kinase gene cluster. *Cell* **86**: 123–133.
- Sarris, P.F., et al. (2015). A plant immune receptor detects pathogen effectors that target WRKY transcription factors. *Cell* **161**: 1089–1100.
- Schell, M.A. (2000). Control of virulence and pathogenicity genes of *Ralstonia solanacearum* by an elaborate sensory network. *Annu. Rev. Phytopathol.* **38**: 263–292.
- Shimono, M., Lu, Y.J., Porter, K., Kvitko, B.H., Henty-Ridilla, J., Creason, A., He, S.Y., Chang, J.H., Staiger, C.J., and Day, B. (2016). The *Pseudomonas syringae* Type III effector HopG1 induces

- actin remodeling to promote symptom development and susceptibility during infection. *Plant Physiol.* **171**: 2239–2255.
- Tanaka, S., Djamei, A., Presti, L.L., Schipper, K., Winterberg, S., Amati, S., Becker, D., Büchner, H., Kumlehn, J., Reissmann, S., and Kahmann, R.** (2015). Experimental approaches to investigate effector translocation into host cells in the *Ustilago maydis*/maize pathosystem. *Eur. J. Cell Biol.* **94**: 349–358.
- Tasset, C., Bernoux, M., Jauneau, A., Pouzet, C., Brière, C., Kieffer-Jacquino, S., Rivas, S., Marco, Y., and Deslandes, L.** (2010). Autoacetylation of the *Ralstonia solanacearum* effector PopP2 targets a lysine residue essential for RRS1-R-mediated immunity in Arabidopsis. *PLoS Pathog.* **6**: e1001202.
- Thapa, S.P., Miyao, E.M., Michael Davis, R., and Coaker, G.** (2015). Identification of QTLs controlling resistance to *Pseudomonas syringae* pv. tomato race 1 strains from the wild tomato, *Solanum habrochaites* LA1777. *Theor. Appl. Genet.* **128**: 681–692.
- Torres, M.A., Dangl, J.L., and Jones, J.D.** (2002). Arabidopsis gp91phox homologues AtrbohD and AtrbohF are required for accumulation of reactive oxygen intermediates in the plant defense response. *Proc. Natl. Acad. Sci. USA* **99**: 517–522.
- Toruño, T.Y., Stergiopoulos, I., and Coaker, G.** (2016). Plant-pathogen effectors: Cellular probes interfering with plant defenses in spatial and temporal manners. *Annu. Rev. Phytopathol.* **54**: 419–441.
- Van Engelenburg, S.B., and Palmer, A.E.** (2010). Imaging type-III secretion reveals dynamics and spatial segregation of Salmonella effectors. *Nat. Methods* **7**: 325–330.
- van Wees, S.** (2008). Phenotypic analysis of Arabidopsis mutants: trypan blue stain for fungi, oomycetes, and dead plant cells. *Cold Spring Harb. Protoc.* **8**: doi/10.1101/pdb.prot498.
- Vasse, J., Frey, P., and Trigalet, A.** (1995). Microscopic studies of intercellular infection and protoxylem invasion of tomato roots by *Pseudomonas solanacearum*. *Mol. Plant Microbe Interact.* **8**: 241–251.
- Vasse, J., Genin, S., Frey, P., Boucher, C., and Brito, B.** (2000). The hrpB and hrpG regulatory genes of *Ralstonia solanacearum* are required for different stages of the tomato root infection process. *Mol. Plant Microbe Interact.* **13**: 259–267.
- Wallden, K., Rivera-Calzada, A., and Waksman, G.** (2010). Type IV secretion systems: versatility and diversity in function. *Cell. Microbiol.* **12**: 1203–1212.
- Wang, G., et al.** (2015). The decoy substrate of a pathogen effector and a pseudokinase specify pathogen-induced modified-self recognition and immunity in plants. *Cell Host Microbe* **18**: 285–295.
- Wang, Q., et al.** (2011). Transcriptional programming and functional interactions within the *Phytophthora sojae* RXLR effector repertoire. *Plant Cell* **23**: 2064–2086.
- Xin, X.F., and He, S.Y.** (2013). *Pseudomonas syringae* pv. tomato DC3000: a model pathogen for probing disease susceptibility and hormone signaling in plants. *Ann. Rev. Phytopathol.* **51**: 473–498.
- Yadeta, K.A., and J Thomma, B.P.** (2013). The xylem as battleground for plant hosts and vascular wilt pathogens. *Front. Plant Sci.* **4**: 97.
- Yang, Q., Li, X., Tu, H., and Pan, S.Q.** (2017). Agrobacterium-delivered virulence protein VirE2 is trafficked inside host cells via a myosin XI-K-powered ER/actin network. *Proc. Natl. Acad. Sci. USA* **114**: 2982–2987.
- Yang, Y., Costa, A., Leonhardt, N., Siegel, R.S., and Schroeder, J.I.** (2008). Isolation of a strong Arabidopsis guard cell promoter and its potential as a research tool. *Plant Methods* **4**: 6.
- Zhou, Z., Wu, Y., Yang, Y., Du, M., Zhang, X., Guo, Y., Li, C., and Zhou, J.M.** (2015). An Arabidopsis plasma membrane proton ATPase modulates JA signaling and is exploited by the *Pseudomonas syringae* effector protein AvrB for stomatal invasion. *Plant Cell* **27**: 2032–2041.

Direct and Indirect Visualization of Bacterial Effector Delivery into Diverse Plant Cell Types during Infection

Elizabeth Henry, Tania Y. Toruño, Alain Jauneau, Laurent Deslandes and Gitta Coaker
Plant Cell 2017;29;1555-1570; originally published online June 9, 2017;
DOI 10.1105/tpc.17.00027

This information is current as of September 5, 2017

Supplemental Data	/content/suppl/2017/07/19/tpc.17.00027.DC2.html /content/suppl/2017/06/09/tpc.17.00027.DC1.html /content/suppl/2017/08/15/tpc.17.00027.DC3.html
References	This article cites 69 articles, 18 of which can be accessed free at: /content/29/7/1555.full.html#ref-list-1
Permissions	https://www.copyright.com/ccc/openurl.do?sid=pd_hw1532298X&issn=1532298X&WT.mc_id=pd_hw1532298X
eTOCs	Sign up for eTOCs at: http://www.plantcell.org/cgi/alerts/ctmain
CiteTrack Alerts	Sign up for CiteTrack Alerts at: http://www.plantcell.org/cgi/alerts/ctmain
Subscription Information	Subscription Information for <i>The Plant Cell</i> and <i>Plant Physiology</i> is available at: http://www.aspb.org/publications/subscriptions.cfm